

# UC Santa Barbara

## UC Santa Barbara Previously Published Works

### Title

Electron mobility in graded AlGaIn alloys

### Permalink

<https://escholarship.org/uc/item/2972c0kb>

### Journal

Applied Physics Letters, 88(4)

### ISSN

0003-6951

### Authors

Rajan, S  
DenBaars, S P  
Mishra, U K  
[et al.](#)

### Publication Date

2006

Peer reviewed

## Electron mobility in graded AlGaN alloys

Siddharth Rajan,<sup>a)</sup> Steven P. DenBaars, and Umesh K. Mishra  
 Department of Electrical and Computer Engineering, University of California, Santa Barbara,  
 California 93106

Huili (Grace) Xing and Debdeep Jena  
 Department of Electrical Engineering, University of Notre Dame, 275 Fitzpatrick, Indiana 46556

(Received 29 September 2005; accepted 15 December 2005; published online 23 January 2006)

Polarization gradients in graded AlGaN alloys induce bulk electron distributions without the use of impurity doping. Since the alloy composition is not constant in these structures, the electron scattering rates vary across the structure. Capacitance and conductivity measurements on field effect transistors were used to find mobility as a function of depth. The effective electron mobility at different depths calculated from theory closely matched the measured mobility. Local bulk mobility values for different AlGaN compositions were found, and the electron mobility in AlGaN as a function of alloy composition was deduced. These were found to match with theoretical calculations. © 2006 American Institute of Physics. [DOI: 10.1063/1.2165190]

Gallium nitride and related alloys have higher spontaneous and piezoelectric polarization than other III-V semiconductors. In AlGaN/GaN heterostructures, the piezoelectric polarization in the strained AlGaN and the discontinuity in the spontaneous polarization at the heterointerface leads to a fixed sheet charge at the heterointerface. This is used in AlGaN/GaN high electron mobility transistors where a two-dimensional electron gas is formed to screen the net positive charge at the AlGaN/GaN junction. The same effect can also be used to create a three-dimensional electron slab<sup>1</sup> (Fig. 1). This is achieved by grading the Al composition in the AlGaN alloy, thus creating a polarization gradient in the graded region. The polarization-induced carrier density,  $\rho_\pi$ , is given by the equation

$$\rho_\pi = \nabla \cdot \mathbf{P}, \quad (1)$$

where  $\mathbf{P}$  is the total polarization in the material. The polarization  $\mathbf{P}$  here is the sum of the spontaneous and piezoelectric polarization in the AlGaN alloy and can be approximated by using Vegard's law for the elastic constants. Transistors based on graded AlGaN alloys have been predicted to be technologically important for microwave applications.<sup>2,3</sup>

In this work, we compare measurements and theoretical calculations of mobility for polarization-induced three-dimensional electron gases in graded AlGaN alloys. The electrical and physical properties vary in the growth direction in graded AlGaN alloys because of the continuously changing Al composition. Electron scattering rates are therefore different in different parts of the channel depending upon the local alloy composition, and these must be taken into account while calculating or analyzing electron mobility in graded alloys.

The effective electron scattering rate (proportional to  $1/\mu_{\text{eff}}$ ) is given by the first moment of the electron density  $[n(z)]$  with respect to the local scattering rate [proportional to  $1/\mu(z)$ ].

$$\frac{1}{\mu_{\text{eff}}(z)} = \frac{\int \frac{n(z)}{\mu(z)} dz}{\int n(z) dz}. \quad (2)$$

Here,  $\mu(z)$  is the mobility for an electron gas of density  $n(z)$  in a bulk AlGaN slab with the composition  $x_{\text{Al}}(z)$ . Calculations for graded AlGaN layers<sup>4</sup> have shown that the dominant scattering mechanisms limiting effective electron mobility at room temperature are alloy scattering and optical phonon scattering. In bulk GaN, Chin *et al.*<sup>12</sup> have shown that optical phonon scattering is the dominant mechanism at room temperatures. In the present work, we therefore take into account only alloy scattering and optical phonon scattering to calculate the bulk mobility in AlGaN alloys

$$\frac{1}{\mu(z)} = \frac{1}{\mu_{\text{op}}(z)} + \frac{1}{\mu_{\text{alloy}}(z)}. \quad (3)$$

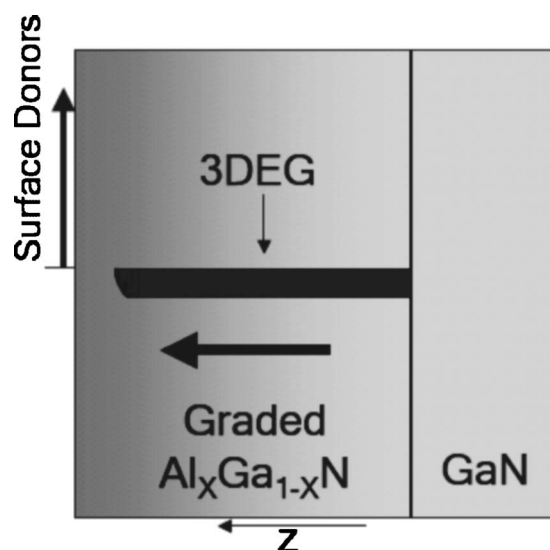


FIG. 1. A three-dimensional electron gas induced in graded AlGaN. The coordinate "z" used in the equations is shown for reference.

<sup>a)</sup>Electronic mail: srajan@ece.ucsb.edu

TABLE I. Material constants for GaN and AlN.

Constant		GaN	AlN	Units	Ref.
Effective mass	$m_e$	0.228	0.35	...	8 and 9
Lattice constant	$a$	3.19	3.11	Å	10
Lattice constant	$c$	5.18	4.98	Å	10
Elastic constant	$c_{13}$	103	108	GPa	11
Elastic constant	$c_{33}$	398	373	GPa	11
Optical phonon energy	$\hbar\omega_{OP}$	91.2	99.2	meV	12
Low frequency dielectric constant	$\epsilon_0$	9.7	8.5	...	13
High frequency dielectric constant	$\epsilon_\infty$	5.3	4.6	...	13

The alloy scattering-limited mobility in an AlGaIn alloy with Al composition  $x_{Al}(z)$  is given by the expression<sup>4</sup>

$$\frac{1}{\mu_{\text{alloy}}(z)} = \frac{2q\hbar kT \ln[1 + \exp(E_f(z)/kT)]}{3\pi m_e(z)V_0(z)^2\Omega_0(z)n(z)x_{Al}(z)[1 - x_{Al}(z)]}. \quad (4)$$

Here,  $V_0$  is the alloy scattering potential for (Al,Ga)N alloys which has been found to be 1.8 eV from magnetotransport measurements on similar structures.<sup>5</sup> The unit cell volume  $\Omega_0(z)$  was calculated for different alloy compositions by linearly interpolating lattice and elastic constants between GaN and AlN, and  $m_e$  is the effective mass of electrons (Table I).  $n(z)$  is the electron density measured by capacitance-voltage (C-V) profiling.  $E_f(z)$ , the position of the Fermi level with respect to the conduction band is found using the Joyce-Dixon approximation<sup>6</sup>

$$E_{fJD} = kT \left[ \ln\left(\frac{n(z)}{N_C(z)}\right) + A1\left(\frac{n(z)}{N_C(z)}\right) + A2\left(\frac{n(z)}{N_C(z)}\right)^2 \right], \quad (5)$$

where the constants A1 and A2 are  $1/\sqrt{8}$  and  $-4.95009 \times 10^{-3}$ , respectively, and  $N_C(z)$  is the conduction band density of states of the AlGaIn alloy in a region with composition  $x_{Al}(z)$ . This was calculated by interpolating between the values (Table I) for AlN and GaN.

The optical phonon scattering rate is given by

$$\mu_{\text{op}} = \frac{4\pi\epsilon_0\epsilon^*(z)\hbar}{qm_e(z)q_0(z)N_{BE}(z)}, \quad (6)$$

where  $\epsilon_0$  is the permittivity of vacuum,  $\epsilon^* = 1/\epsilon_0(z) - 1/\epsilon_\infty(z)$ ,  $m_e(z)$  is the electron effective mass,  $q_0(z)$  is the optical phonon energy, and  $N_{BE}(z)$  is the Bose-Einstein phonon number in an AlGaIn alloy with composition  $x_{Al}(z)$ . The constants for the AlGaIn alloy were calculated by linear interpolation between the respective values for AlN and GaN (Table I).

The structure used in these experiments was grown on a sapphire substrate by metalorganic chemical vapor deposition. It consists of an insulating GaN buffer,<sup>7</sup> an AlGaIn region linearly graded from 0% to 30% over 100 nm and a 5 nm GaN layer. Transistors and capacitors were fabricated on this epilayer using standard processing techniques. Ti/Al/Ni/Au contacts were deposited and annealed at 870 °C for 30 s, mesa isolation was achieved using Cl<sub>2</sub>-based reactive ion etching, and a Ni/Au metal layer was deposited for gate contacts.

Electron mobility in these structures were measured using a combination of transistor  $I$ - $V$  measurements and C- $V$

profiling. First, the charge as a function of depletion distance,  $n(z)$ , was calculated from C- $V$  measurements, as shown in Fig. 2. Since this structure was not doped, the total integrated charge for depletion depth can be related to the the composition at that depth using Eq. (1). The calculated composition versus depth profiles (Fig. 2, inset) are used in the theoretical calculations of mobility.

A small current (100  $\mu$ A) was forced between the source and drain of the transistor for different gate voltages and the voltage drop between source and drain ( $V_{DS}$ ) was recorded. The voltage drop in the channel region under the gate is given by

$$V_{CH} = V_{DS} - I_{DS}(R_S + R_D). \quad (7)$$

The source and drain access resistances,  $R_S$  and  $R_D$  were estimated using the sheet resistance and contact resistance estimated from transfer length method measurements. Since a very small current was applied, we assume that the lateral electric field and charge distribution under the gate is uniform. With this assumption, the mobility at any gate voltage  $V_G$  is given by the equation

$$\mu_n(V_G) = \frac{I_{DS}}{qn_s(V_G)\left(\frac{V_{DS}}{L_g}\right)}, \quad (8)$$

where  $n_s$  is the total sheet charge at a gate bias  $V_G$  (calculated from C- $V$  measurements) and  $L_g$  is the gate length (0.7  $\mu$ m). Since the depletion depth at each gate voltage is known from C- $V$  profiling, the mobility as a function of depletion depth can be calculated. Measured and calculated electron mobilities for different depletion depths, shown in Fig. 3, show good agreement. As expected the channel has the highest mobility close to depletion where most of the charge is in low composition AlGaIn and there is less alloy scattering.

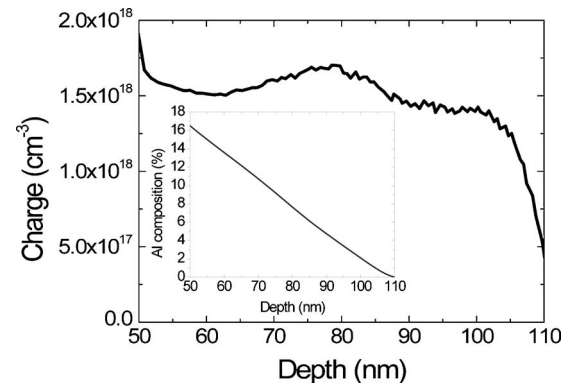


FIG. 2. Carrier concentration vs depth. The inset shows the calculated Al composition at each depth.

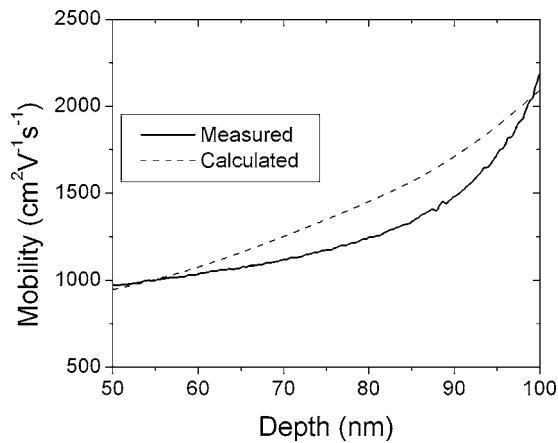


FIG. 3. Mobility vs depletion depth from theory and simulations (300 K).

These measurements also confirm measurements of the alloy scattering potential by Jena *et al.*<sup>5</sup>

The information from these measurements can also be used to calculate the mobility as a function of Al composition. Equation (2) can be rearranged and discretized to give

$$\frac{n_K}{\mu_K} = \frac{n_{s,K-1}}{\mu_{\text{eff},K}} - \frac{n_{s,K}}{\mu_{\text{eff},K-1}} \quad (9)$$

where  $n_{s,K}$  is the integrated sheet carrier densities in the undepleted region upto the  $K$ th region,  $\mu_{\text{eff},K}$  is the effective mobility of that sheet, and  $n_K$  is the sheet charge in the  $K$ th discrete region. Therefore, since the effective mobility at different depletion depths and the associated sheet charge are known, the *bulk* mobility for the Al composition at each of these points can be calculated.

The mobility values calculated using this method are compared with the theoretical bulk mobility [from Eq. (3)] in Fig. 4. The alloy and optical phonon-limited mobilities from

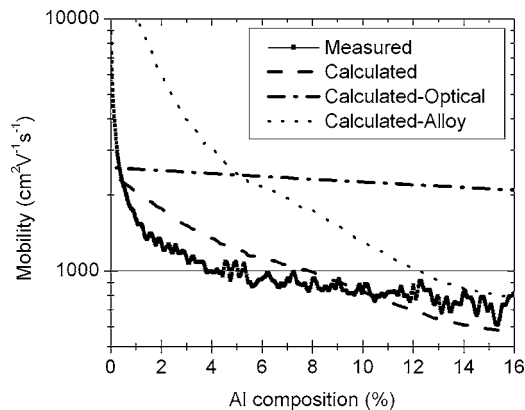


FIG. 4. Bulk AlGaIn mobility from theory and simulations (300 K).

theory are also shown. At lower Al compositions, the mobility is limited mainly by optical phonon scattering whereas at Al compositions greater than around 0.14 the mobility is mainly alloy-scattering limited. At very low GaN compositions (below 0.5%) the measured mobility shown in the plot is higher than the calculated mobility. The measurement in this regime may be affected by variations in the epitaxial layers between the  $C$ - $V$  patterns and the transistors. Further, since the sheet density is low and the lateral electric fields are high, the simple relations applied to calculate the mobility are no longer valid. At higher Al compositions, however, there is a good match between the measured and theoretical values of mobility.

In conclusion, the effective mobility as a function of depletion depth in graded AlGaIn alloys was calculated taking into account alloy and optical phonon scattering. Experimental mobilities were estimated using transistor  $I$ - $V$  and capacitance-voltage measurements. A good match was found between the experimental and theoretical values. The bulk AlGaIn mobilities as a function of alloy composition were also estimated from these measurements and were found to agree well with the theoretically predicted values. The mobility characterization may be used in the analysis and design of transistors based on these graded AlGaIn layers.

The authors thank Y. Dora, T. Palacios, and D. Buttari for discussions. The authors acknowledge funding from CNID and from the Office of Naval Research under a grant monitored by Dr. Harry Dietrich.

<sup>1</sup>D. Jena, S. Heikman, D. Green, D. Buttari, R. Coffie, H. Xing, S. Keller, S. Denbaars, J. S. Speck, and U. K. Mishra, *Appl. Phys. Lett.* **81**, 4395 (2002).

<sup>2</sup>S. Rajan, H. Xing, D. Jena, S. P. Denbaars, and U. K. Mishra, *Appl. Phys. Lett.* **84**, 1591 (2004).

<sup>3</sup>S. Rajan, H. Xing, A. Chakraborty, A. Chini, M. J. Grundmann, T. Palacios, D. Jena, S. P. Denbaars, and U. K. Mishra, *International Workshop on Nitride Semiconductors, July 2004, Pittsburgh PA, Conference Abstract*.

<sup>4</sup>D. Jena, Ph.D. thesis, University of California, Santa Barbara, CA, 2002.

<sup>5</sup>D. Jena, S. Heikman, J. S. Speck, A. Gossard, U. K. Mishra, A. Link, and O. Ambacher, *Phys. Rev. B* **67**, 153306 (2003).

<sup>6</sup>W. B. Joyce and R. W. Dixon, *Appl. Phys. Lett.* **31**, 354 (1977).

<sup>7</sup>S. Heikman, S. Keller, S. P. Denbaars, and U. K. Mishra, *Appl. Phys. Lett.* **81**, 439 (2002).

<sup>8</sup>L. W. Wong, S. J. Cai, R. Li, K. Wang, H. W. Jiang, and M. Chen, *Appl. Phys. Lett.* **73**, 1391 (1998).

<sup>9</sup>K. Kim, W. R. L. Lambrecht, B. Segall, and M. van Schilfgaarde, *Phys. Rev. B* **56**, 7673 (1997).

<sup>10</sup>O. Ambacher, *J. Phys. D* **31**, 2653 (1998).

<sup>11</sup>A. F. Wright, *J. Appl. Phys.* **82**, 2833 (1997).

<sup>12</sup>V. W. L. Chin, T. L. Tansley, and T. Osothchan, *J. Appl. Phys.* **75**, 7365 (1994).

<sup>13</sup>*NSM Archive—Physical Properties of Semiconductors*, <http://www.ioffe.rssi.ru/SVA/NSM/Semicond>, and references therein.